How roughness emerges on natural and engineered surfaces

Ramin Aghababaei,* Emily E. Brodsky, Jean-François Molinari, and Srinivasan Chandrasekar

Roughness, defined as unevenness of material surfaces, plays an important role in determining how engineering components or natural objects interact with other bodies and their environment. The emergence of fractal roughness on natural and engineered surfaces across a range of length scales suggests the existence of common processes and mechanisms for nucleation and evolution of roughness. In this article, we review recent advances in understanding the origins of roughness and topography evolution on natural and engineered surfaces and their connection with subsurface deformation mechanisms. Directions for future research toward understanding the origins of roughness on solid surfaces are discussed.

Introduction

Surface roughness, also referred to as surface topography, is the degree of unevenness of solid surfaces. It appears on every natural and engineered surface and across multiple length scales ranging from atomic to tectonic.[1] There are many methods (e.g., frequency distributions, fractal analysis, and surface curvature) to measure surface roughness mathematically. Understanding the origins of roughness at different length scales is of great interest for many scientific fields as it directly influences key mechanical, tribological, chemical, and optical properties of materials and components.

At microscopic scales, the surface roughness of engineering components is dictated by the manufacturing processes used to produce the component (e.g., machining, lapping, grinding, and additive manufacturing) as well as running conditions (e.g., contact and loading conditions, temperature). On the other hand, functional properties of the components such as noise, run-in behavior, product durability, and optical characteristics are to a large extent governed by the surface roughness parameters.[2] At large tectonic scales, the topography of a geologic fault exposed at the surface of the Earth may have an influence on the size of seismic events.[3] Similar to engineering components, field investigations of faults indicate that each surface experiences mechanical wear during relative motions between opposing sides of faults. Understanding the physics and mechanics of roughness evolution during sliding contact between solid surfaces can help provide answers to many important questions such as what is the correlation between the fault roughness and magnitude of earthquakes, what are the origins of unique Hurst exponents for certain classes of materials, or what manufacturing methods should be employed to achieve desired surface topography and, by extension, product performance?

It has long been known that roughness emerges from a complex interplay between dissipative mechanical mechanisms (e.g., visco-elasticity,[4] plasticity,[5,6] fracture,[7,8] wear,[9,10] erosion[11]) and chemical processes (e.g., corrosion[12]). Roughness measurements on surfaces of a wide range of natural materials and engineering components have shown that there exists a fractal roughness with a statistical self-affine scaling across multiple length scales.[1,11] This indicates the existence of common processes and mechanisms that dictate the roughness evolution across all scales. For instance, fracture dominates roughness creation on large-scale faults whereas plasticity governs roughness of small-scale faults. Similarly, but at much smaller scales, plasticity is of interest to achieve a smooth material

Ramin Aghababaei, Department of Mechanical and Production Engineering, Aarhus University, Aarhus, Denmark; ra@mpe.au.dk
Emily E. Brodsky, Earth and Planetary Sciences, University of California, Santa Cruz, Santa Cruz, USA; brodsky@ucsc.edu
Jean-François Molinari, Department, Institute of Civil Engineering, Institute of Materials, Ecole Polytechnique Fédérale de Lausanne (EPFL), Lausanne, Switzerland; jean-francois.molinari@epfl.ch
Srinivasan Chandrasekar, School of Industrial Engineering, Purdue University, West Lafayette, USA; chandy@purdue.edu
*Corresponding author

doi:10.1557/s43577-022-00469-1

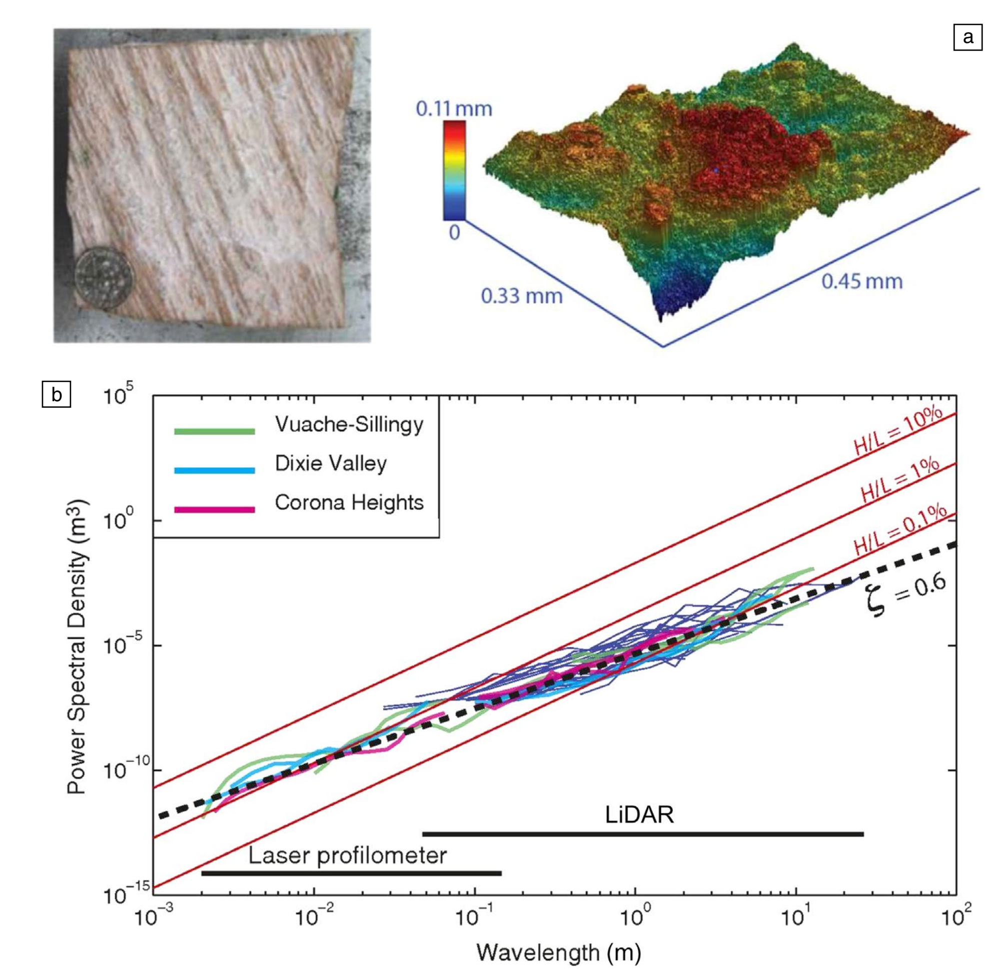

Figure 1. (a) The minimum scale of grooving as visualized in a grooved fault sample from Mount St. Helens and a white-light interferometric image of the same surface that show isotropic roughness at submillimeter scales. (b) Power spectral density data obtained from three individual faults (Vuache-Sillingy, France; Dixie Valley, Nev., USA; Corona Heights, Calif., USA),[15] suggesting that faults are rougher at small scales in the slip direction.

removal and a high-quality surface finish in cutting processes, whereas fracture-induced chip breaking is of equal importance to prevent the formation of long chips. Despite these similarities, an agreed-upon understanding of how roughness emerges on natural and synthetic surfaces has remained elusive. The main reason is that *in situ* experimental tracking as well as direct simulation of roughness creation and evolution at contacts between solid surfaces present substantial challenges.[13,14]

In this review, we present recent advances and trends toward understanding the emergence of roughness on natural and engineered surfaces. We discuss the influence of subsurface deformation mechanisms such as plasticity and fracture at small scales on the emergence of roughness on geological faults and metallic components produced by different manufacturing processes, as well as the evolution of roughness during sliding contact.

Natural surfaces

Earthquakes are one of the most dramatic examples in nature of sliding contact and frictional failure. The resulting faults also provide some of the best evidence for the existence of steady-state, scale-dependent roughness.[15,16] The topography of geologic fault surfaces exposed at the surface of the Earth has been measured using a variety of tools, including mechanical profilometers, ground-based LiDAR, and stereoscopy.[16–19] **Figure 1**a shows small hand samples that have been brought into the laboratory and measured at even finer resolution using AFM and white-light interferometry.[20,21]

In aggregate, the data have revealed clear systematic trends. As could be expected, slip-perpendicular roughness is generally larger than slip-parallel roughness. Interestingly, the slip-perpendicular roughness can be similar to that of unslipped, unworn crack faces in rocks and generally does not evolve much with slip.[18] The slip-parallel roughness does decrease with moderate (<10 *m* slip), but then appears to not evolve significantly after a fault has moved large distances (>100 *m*). The resulting power spectral densities for different mature faults are restricted to a range of values that vary by less than an order of magnitude at a given wavelength.[15] Although this may seem like a large spread in values to an engineer, it is a relatively tight range for a geological observation given the range of rock types, faults, and ambient conditions involved. Typically, the power spectral density of a fault can be fit in the slip-parallel with Hurst exponent of 0.6, which implies that the aspect ratio H/L of asperities increases with decreasing scale where H is the root-mean-square (RMS) height of surface topography measured at scale L. In this sense, faults are rougher at small scales than large ones (Figure 1b).

We can potentially explain the systematic trends by thinking about the fault as preserving a steady-state roughness that is governed by the strength of rocks. Earthquakes have repeatedly slipped the fault-driving asperities against each other and causing ones that are too high or steep to break. In an order-magnitude sense, the shear strain required to elastically deform one asperity enough to slip past a similarly sized one is H/L because asperities of height H need to be flattened and that displacement is supported over the asperity width L.[15] If this shear strain exceeds the critical strain in a material, the asperity will break and not be preserved. Thus, an upper limit of the preserved roughness may be controlled by the strength of the material. A steady-state roughness can be achieved if competing, re-roughening processes such as plucking and fracturing continually create new roughness and drive the surface topography to the strength-controlled limit.

The rock record provides some support of this interpretation of preserved roughness as reflective of bulk material strength. The preserved roughness has larger values of H/L at small scales, which would be consistent with the common observation that rocks (and many other materials) are stronger at small scales than large ones. Quantitatively, the roughness at extremely small scales on a few samples has been correlated directly with the size-dependence of indentation-derived measurements of strength.[21] At larger scales, the Hurst exponent of 0.6 translates to the aspect ratio H/L (and hence strength) decreasing as $L^{-0.4}$. The dependence here is suggestively close to the inverse square root dependence of strength long suggested for rocks.

The previously discussed interpretation suggests a way to infer scale-dependent strength of materials from observations of steady-state roughness. If correct, ceramics and other materials could be characterized at a range of scales by doing large-slip wear experiments such as those possible in large-scale rotary shear apparati (see also the subsection on "Adhesive sliding and three-body contact").

These systematic trends hold on faults to the largest scales yet observed.[16,22,23] However, at small scales, a different phenomenon is observed. Between 1 and 100 microns, the slip-parallel and slip-perpendicular roughness of natural and laboratory fault surfaces start to overlap.[20] At even smaller scales, the faults are no longer grooved, but rather isotropic in their roughness. This minimum scale of grooving varies from fault to fault and even between locations on a single fault. However, for each observed fault the aspect ratio H/L at which the minimum scale of grooving is observed is well-defined.[20]

The importance of the aspect ratio is consistent with the interpretation of H/L as reflective of the strength of the material. In the case of the minimum scale of grooving, the scale may be defining a crossover between the brittle strength, which governs the large-scale roughness, and the plastic strength, which governs the small-scale roughness. The minimum scale of grooving may therefore be an observational manifestation of a brittle-plastic transition as a function of scale. Small-scale asperities are deformed plastically. This is consistent with longstanding interpretations of friction as generated by the interaction and cooperative accommodation of the load by elastoplastic topography.[24] The maximum scale of these plastic contacts can be related to the slip weakening distance D_c often invoked in rate-state friction[25] (see also the article by Weber et al.[26]). At larger scales, asperities break by brittle failure. A similar ductile-to-brittle transition has been recently suggested for failure of asperity junctions during adhesive sliding[27] and chips formation in abrasive processes[28] (see "Abrasive processes and material removal" section).

This interpretation of the minimum scale of grooving is supported by comparing the scale on different rock types.[29] Carbonate rocks, which are more plastic, have smaller minimum scales of grooving than silica ones. By using the Lawn and Marshall formulation[30] of the minimum crack size that can propagate by brittle means as a proxy for the brittle-ductile transition, one can predict the ratio of minimum scales of grooving based on the critical stress intensity factors and plastic yield strengths of each material. The resulting ratio of predicted minimum grooving sizes is consistent with this observation.

Natural faults have provided evidence that surfaces can develop steady-state wear that may be reflective of the scale-dependent strength of the material. This interpretation has yet to be applied to engineered materials or utilized in more general contexts. Likely, a firmer theoretical foundation is necessary as well as specifically designed experiments that test the generality of the hypothesis across materials.

Engineered surfaces

Unlike in faults, where the interface is typically between two rocks of the same type and thus properties, in manufacturing a higher-hardness die or cutting tool is imposing deformation onto a lower-hardness metal workpiece. In this article, we focus on metals as the materials system, and metal component manufacturing processes widely used in the discrete products manufacturing sector. Large-strain plastic deformation and, to a lesser extent, ductile fracture, play an important role in the surface topography evolution in these processes. The observations and lessons learned will be of value also for other material systems (e.g., ceramics, polymers) wherein similar processes are employed, and the underlying material phenomena are similar, varying only in degree.

Bulk deformation processing

To understand surface topography in forming processes like rolling and extrusion, we begin with a well-known picture from the early days of tribology—a cross section of a deep indentation made on the surface of annealed copper imprinted with fine grooves (see References 31 and 32. The picture shows that the grooves (asperities) on the surface are essentially unchanged, even after the deep indentation. This observation is intriguing given that one would expect the grooves to deform plastically at these indentation pressures, which locally are on the order of 1 to 3 σ_y (σ_y is yield strength of the metal). However, it is only when the pressure

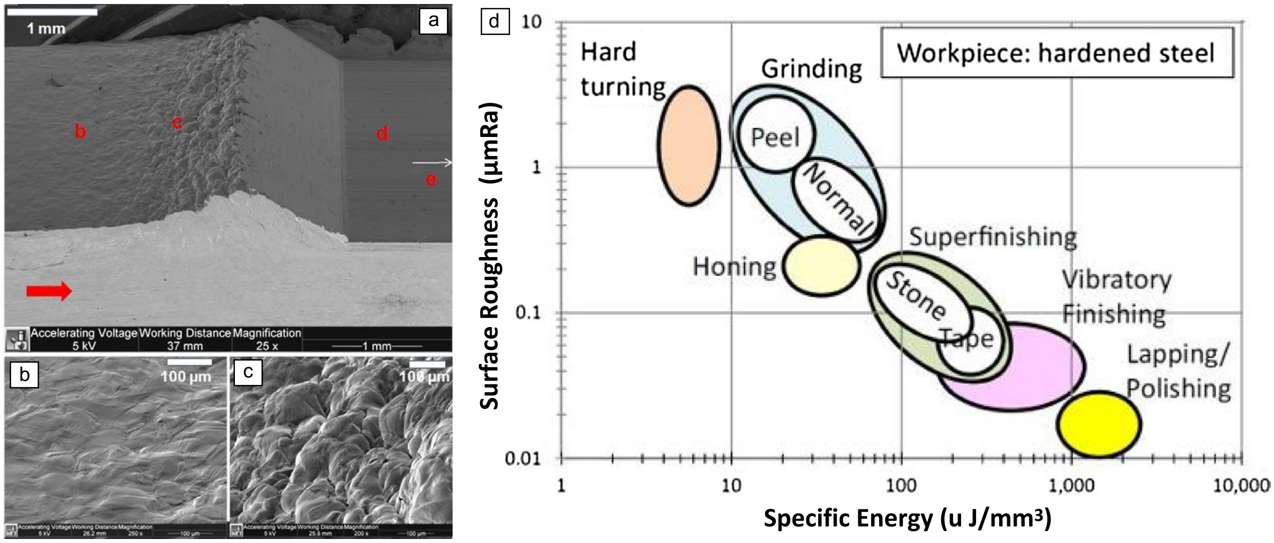

Figure 2. (a) Scanning electron microscope image of the workpiece surface in wedge sliding. The stationary wedge (not shown) is located in regions "d" and "e," where the workpiece moves from left to right (adapted from Reference 43). (b, c) Displacement of surface grains in regions "b" and "c," illustrating the emergence of surface roughness by differential grain deformation "ahead" of the wedge (a similar process occurs in sheet-metal forming). (d) Dependence of surface roughness, Ra, on specific energy for various material removal processes; from machining (turning) to abrasive finishing processes.[44]

is increased, so that bulk plastic flow occurs and this plastically deformed region grows to encompass the surface, that the asperities are found to flatten out.[33]

In rolling of foil and sheet, the die-workpiece contact pressures are sufficiently large that bulk (homogeneous) deformation occurs in the sheet and encompasses the sheet surface, especially in the latter cold-rolling stages of the processing.[34] Consequently, any asperities initially present on the sheet surface are fully flattened. This also illustrates a fundamental characteristic of the tribology of die-workpiece interfaces in bulk deformation processing and cutting: in contrast to conventional sliding contacts, the contact conditions at the process interfaces are characterized by intimate contact between die and workpiece, very high stresses, and real area of contact equal to the apparent (geometric) area.[32,34,35] Under such conditions, the product surface, which is fully constrained by contact with the die, develops a topography that is a replica of the die surface at typical engineering length scales (to 0.5 to 1 µ*m*). This is confirmed by topography observations on rolled/extruded products, including Al foil;[36–38] underside of machining chips, which are in intimate contact with the tool; and contact roll-to-roll printing (e.g., gravure process[39]). Microstructure plays essentially no role, under these constrained deformation conditions, in influencing the surface topography. Taken together, the observations suggest that in forming processes where the surface deformation is fully constrained by contact with a die, the product surface topography is essentially a replica of the die surface. This opens up the possibility of achieving high-quality surface finish and controlled topography in formed products by control of the die texture, even without use of other secondary processes. It also suggests opportunities for using textured indenters and quasistatic indentation loading to understand surface topography evolution in constrained forming processes.

Sheet-metal forming

At the other end of the spectrum, in terms of constraint on deformation geometry, are sheet-forming processes such as bending and stretching. Here, the surface is essentially unconstrained (plane stress) and free to displace along the surface normal direction during the deformation. In such unconstrained deformation, the surface topography development is dominated by deformation (strain and strain localization) and microstructure (grain size and crystallographic texture) effects[40–42] even though the forming strains are significantly lower than in the bulk forming processes. The notable topography features that arise in are the well-known "orange peel" roughness and roping/ridging, both undesirable in sheet-metal products.

The orange peel is roughening on the order of the grain size due to differential deformation of the grains.[45] An example of this type of microstructure-induced roughness, albeit on the free surface ahead of a sliding wedge wherein the deformation and field is similar to sheet forming, is shown in **Figure** 2. The surface grains on the free surface have undergone differential deformation due to crystallographic anisotropy and flow stress variations. The differential deformation is manifested as equiaxed roughness features that scale approximately with the grain size. The extent of this roughness typically increases with increasing strain and grain size, occurrence of strain localization, and reduction in slip systems. This dependence of the roughness on strain is also seen in Figure 2b–c: the grains in the more highly strained region immediately ahead of the wedge exhibit greater surface displacements than in regions farther away. This figure also illustrates the key aspect of surface roughness in bulk forming processes—the workpiece surface being a replica of the die surface. The inclined region (to the left of region d in Figure 2a), which is the region in contact with the wedge, is seen to be smooth and is a replica of the wedge surface. The roping topography phenomenon is also microstructure-driven, except that it involves the formation of surface corrugations, due to clusters of grains having different orientations and resulting deformation anisotropy.[45,46] Not surprisingly, similar roughening due to subgrain deformation has been observed even in single crystals.[6,47,48]

Abrasive processes and material removal

Material removal during abrasive processes such as machining, grinding, and polishing play an extraordinary important role in determining the surface topography in engineering components. Understanding of the topography evolution is still in its infancy with the surface generation typically being described in textbooks as arising from geometric tool motions. However, there are various attributes of these processes (beyond tool motions) that are critical for topography evolution, and which warrant study.

First, as nicely illustrated in Figure 2d, the undeformed chip thickness (h_{eq}), (or the cutting depth in an orthogonal cutting setup), which is the key parameter controlling the degree of material removal, plays a critical role in determining the surface finish. Across a broad class of machining and finishing processes, the component roughness, Ra, is seen to decrease with decreasing h_{eq}.[44,49] But concurrently, the process specific energy (i.e., the energy required to remove a unit volume of material) also increases[44]—processes that give rise to smooth surfaces are also highly energy-intensive, the energy increasing by as much as three orders of magnitude between simple cutting and very fine abrasive (grit) processes. When the undeformed chip thickness (h_{eq}) is smaller (i.e., approaching or less than the tool/abrasive-particle edge radius), the frictional energy dissipation (arising from ploughing and rubbing) becomes more significant relative to the energy purely associated with material removal chip formation. Because the ploughing and rubbing only result in material displacement, not material removal, the specific energy increases with decreasing h_{eq}. But the gains in surface finish (e.g., Ra) are quite spectacular—with up to three orders of magnitude improvement (see Figure 2d), albeit at the expense of energy cost!

Second, the deformation zone in these processes is partially constrained with the new surface forming typically in the wake of a sliding tool. Observations show that the topography development in machining processes is strongly influenced by the plastic flow mode controlling chip formation[50]—uniform deformation versus nonuniform flow (e.g., sinuous, shear bands). Flow modes associated with lower forces give rise to much better surface finishes. A recent study[28] revealed the existence of a critical cutting depth, below which the chip formation is dominated by plastic deformation, and above which chips break off by crack propagation. This observation highlights the importance of the chip formation mechanism on the final surface finish.[51] As to why/how the flow mode is able to influence the topography of the new surface that is generated in the wake of the tool is an unresolved question.

Third, the RMS surface parameters evolve monotonically to their steady-state condition in abrasive processes (e.g., polishing, superfinishing) without any overshoot or oscillation. The steady-state roughness value, which is a function of the abrasive grit size and applied pressure (loading), can be greater or less than the initial workpiece roughness.[52] This latter fact is not so well known as it is often implicitly assumed, for example during polishing, that the surface will always become smoother. Although the material removal mechanism underlying the surface generation often involves significant surface plasticity, be it in ductile or brittle solids, it is interesting that one can broadly formulate a model for the topography evolution in these abrasive processes without detailed consideration of the mechanics of material removal. This may be done by analogy with stone and pebble erosion[53–55] by postulating that the local material removal rate on the surface is related to the local curvature of the asperities, that is, "sharp points" get smoothed out faster than other less sharp neighboring regions. Such a model (unpublished work) can predict many features of the topography evolution in abrasive and erosion processes, including material removal rates and the process time constant.

Adhesive sliding and three-body contact

Once engineering components have been manufactured, many of them, such as the rocks discussed in the beginning of this article, undergo sliding contact during use, which causes further evolution in their surface topography. It is long known that surface roughness controls tribological properties, but much less is known how roughness evolves with time. For various engineering surfaces in sliding contact, the roughness is found to converge to a steady-state value.[56–58] Both friction and wear have a profound influence on the emerging roughness.

As detailed in the section "Abrasive processes and material removal," abrasive processes substantially affect roughness. A hard material generates a groove when it scratches a soft material, to the dismay of car owners, who would rather avoid scratches, but to the benefit of polishing technology where finer and finer grits are used to smoothen large asperities. Although generally one has an intuitive understanding on how abrasive wear affects roughness, much less is clear when dealing with the most prominent form of wear, adhesive wear, which is the result of the transference of material from one surface to another due to adhesive forces.

Recently, Milanese et al.[14] have conducted molecular dynamics (MD) simulations of sliding materials in dry contact and in the presence of strong adhesive interactions. These simulations revealed that the surface roughness reaches a steady state. The simulations (see **Figure 3**) used a periodic simulation box in the sliding direction so that the contact surface was worked several times, as one would expect in

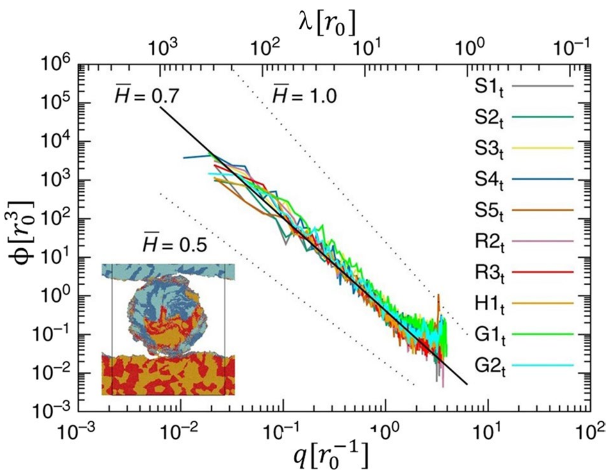

Figure 3. Power spectra density (PSD) of the surface roughness after a rolling debris generated via molecular dynamics (MD) simulations (adopted from Reference 14). The PSD reveals a universal feature of the surface roughness, with a Hurst exponent, $\bar{H}$, around 0.7, although the high computational cost of MD simulations limited this observation to only two orders of magnitude in length scale. The different colors represent different initial roughness (see Reference 14 for more details), and show that the emerging roughness has some universal features for the class of material studied here. The inset shows the snapshot of MD simulation, which revealed the creation of a rolling debris.

a tribological contact. A key element to reach a steady-state roughness was the ability for those simulations to give birth to adhesive debris particles, which is particularly challenging in atomistic simulations. Aghababaei et al.[27,59] were the first to reproduce with computer simulations the adhesive wear mechanism, which was postulated by Rabinowicz.[57] A critical element is to use a simulation box size and a contact junction size between colliding asperities both large enough, in order to generate crack propagation and the formation of a third body. One can correlate this result to the development of steady-state wear observed on surfaces of natural faults.[15,29] This work resulted in the observation of a critical junction size (recently confirmed by *in situ* experiments[60]), function of materials properties, above which debris can be generated by fracture, and below which plastic smoothening of the asperities occurs.[61,62] This can explain the minimum scale of grooving observed on rocks[20] as a result of ductile-brittle transition in asperities failure (also see the section "Natural surfaces").

Once a debris particle is generated, the surface roughness evolves due to two competing mechanisms. These are, on the one hand, a smoothening mechanism during which the third body pushes plastically protruding asperities that are in its path, and on the other hand a roughening mechanism during which strong adhesive forces lead to occasional crack propagation and detachment of matter.[14,63,64] Remarkably these two competing mechanisms led to a steady-state roughness, with a power spectral density displaying features reminiscent of self-affine fractal surfaces. For the class of materials investigated (simple Morse pair potential), irrespective of initial roughness of the contacting surfaces, the surfaces all evolved to a Hurst exponent of about 0.7 (Figure 3).

The critical junction size, which gives rise to a minimum particle size, helps understand the first instants of gouge or third body creation.[27,64] The emergence of surface roughness and gouge has since then been observed with pin-on-disk experiments.[65] It was shown that nanoscale ceramic debris are created at an SiO_2/Si or Si/Si interface, accumulate mass, and elongate into cylindrical debris (also observed with MD simulations[66]), to finally agglomerate in flakes forming a rather complex and heterogeneous third body layer, whose properties deeply influence tribological performance.

Much more needs to be understood from sliding contact between rough surfaces. How and at what rate are debris evacuated for the contact? Why did the material class studied yield the emergence of a Hurst exponent of 0.7, and not something closer to a random walk roughness ($\bar{H} = 0.5$)? Time-dependent adhesion between the contacting surfaces is also an important parameter but which brings unique challenges because a reduced adhesion slows down the evolution to self-affinity as the debris particles spend more time sliding than rolling (relative to the full adhesion case).

Summary and perspective

In this article, we reviewed recent advances and findings on the emergence of roughness on natural and engineered surfaces, focusing on a common feature: self-affine fractal roughness. The appearance of fractal roughness on all natural and engineered surfaces, independent of materials, environmental conditions, and scales, indicates the existence of common deformation mechanisms that create roughness at all scales. Most surfaces, however, exhibit different (scale-dependence) roughness parameters that can be associated with disparate contributions from all deformation mechanisms that shape surfaces, among which plasticity and fracture are the most prominent.

For instance, it is observed that fault surfaces are rougher at smaller scales. This scale-dependent roughness can be understood as arising because brittle fracture (i.e., abrupt crack propagation) governs the roughness creation at macroscopic scales, whereas plastic deformation controls the evolution of faults roughness at microscopic scales. This makes sense because material strength is scale-dependent.[67] Similarly, the roughness of engineering components is a direct result of mechanisms and processes that control material shaping or removal during manufacturing processes. A direct correlation between roughness and materials fracture and yield strengths suggests roughness measurement as a potential characterizing tool to obtain materials fracture and plasticity properties at different scales.

Given the clear connection between surface roughness features and materials properties and microstructure, there is scope for using simulations and analytic models to study roughness development and scaling associated with these patterns. A possible approach involves coupling of local crystal plasticity modeling,[41] with continuum modeling of grain-level deformation (incorporating flow stress anisotropy).[42,43] The latter modeling can capture the deformation over sufficiently large (few millimeter) regions, which is essential for analyzing surface texture development. Alternatively, discrete approaches such as molecular dynamics, discrete dislocation dynamics, and discrete particle/element methods can be used to monitor roughness development at nano- and microscales.

Acknowledgments

We would like to thank L. Pastewka and T. Jacob for their thoughtful efforts and comments toward improving this manuscript. R.A., E.B., and J.F.M. acknowledges respectively the support from the Innovation Fund Denmark (Cutting Edge, 8090-00010B), United States NSF EAR-1624657, and the Swiss National Science Foundation (Wear across scales, 200021-197152). S.C. acknowledges United States NSF Grants DMR 2104745 and CMMI 2100568 to Purdue University used in partial support of this work.

References

1. B. Mandelbrot, *Science* **156**(3775) (1967)
2. H. Dagnall, *Exploring Surface Texture* (Rank Taylor Hobson, Leicester, 1986)
3. O. Zielke, M. Galis, P.M. Mai, *Geophys. Res. Lett.* **44**(2), 777 (2017)
4. R. Vacher, A.S. de Wijn, *Materials* (Basel) **14**(23) (2021)
5. K. Balusu, R. Kelton, E.I. Meletis, H. Huang, *Mech. Mater.* **134**, 165 (2019)
6. A.R. Hinkle, W.G. Nöhring, R. Leute, T. Junge, L. Pastewka, *Sci. Adv.* **6**(7), 0847 (2020)
7. E. Bouchaud, J.-P. Bouchaud, *Phys. Rev. B* **50**, 17752 (1994)
8. Z. Wang, Y. Bao, J.-M. Pereira, E. Sauret, Y. Gan, *Phys. Rev. Fluids* **7**, 024101 (2022)
9. K.J. Kubiak, T.W. Liskiewicz, T.G. Mathia, *Tribol. Int.* **44**(11), 1427 (2011)
10. C.Q. Yuan, Z. Peng, X.P. Yan, X.C. Zhou, *Wear* **265**(3), 341 (2008)
11. B.N.J. Persson, *Tribol. Int.* **54**, 99 (2014)
12. A. Toloei, V. Stoilov, D. Northwood, "The Relationship Between Surface Roughness and Corrosion," in *Proceedings of ASME International Mechanical Engineering Congress and Exposition, Volume 2B: Advanced Manufacturing* (2013), paper no. IMECE2013-65498
13. T.D.B. Jacobs, C. Greiner, K.J. Wahl, R.W. Carpick, *MRS Bull.* **44**(6), 478 (2019)
14. E. Milanese, T. Brink, R. Aghababaei, J.-F. Molinari, *Nat. Commun.* **10**(1), 1116 (2019)
15. E.E. Brodsky, J.D. Kirkpatrick, T. Candela, *Geology* **44**(1), 19 (2016)
16. T. Candela, F. Renard, Y. Klinger, K. Mair, J. Schmittbuhl, E.E. Brodsky, *J. Geophys. Res.* **117**, 8409 (2012)
17. W. Power, T. Tullis, J. Weeks, *J. Geophys. Res.* **93**(B12), 15268 (1988)
18. A. Sagy, E.E. Brodsky, G. Axen, *Geology* **35**(3), 283 (2007)
19. K.A.H. Shervais, J.D. Kirkpatrick, *J. Struct. Geol.* **91**, 130 (2016)
20. T. Candela, E.E. Brodsky, *Geology* **44**(8), 603 (2016)
21. C.A. Thom, E.E. Brodsky, R.W. Carpick, G.M. Pharr, W.C. Oliver, D.L. Goldsby, *Geophys. Res. Lett.* **44**(18), 9299 (2017)
22. J.H. Edwards, J.W. Kluesner, E.A. Silver, E.E. Brodsky, D.S. Brothers, N.L. Bangs, J.D. Kirkpatrick, R. Wood, K. Okamoto, *Nat. Geosci.* **11**(3), 197 (2018)
23. J.D. Kirkpatrick, J.H. Edwards, A. Verdecchia, J.W. Kluesner, R.M. Harrington, E.A. Silver, *Nat. Geosci.* **13**(5), 369 (2020)
24. F.P. Bowden, D. Tabor, *The Friction and Lubrication of Solids* (Oxford University Press, Oxford, 1950)
25. J. Dieterich, B. Kilgore, *Pure Appl. Geophys.* **143**(1), 283 (1994)
26. B. Weber, J. Scheibert, M.P. de Boer, A. Dhinojwala, *MRS Bull.* **47**(12) (2022). https://doi.org/10.1557/s43577-022-00464-6
27. R. Aghababaei, D.H. Warner, J.-F. Molinari, *Nat. Commun.* **7**(1), 11816 (2016)
28. R. Aghababaei, M. Malekan, M. Budzik, *Phys. Rev. Lett.* **127**, 235502 (2021)
29. K.K. Okamoto, E.E. Brodsky, C.A. Thom, L. Smeraglia, A. Billi, *Geophys. Res. Lett.* **46**(21), 11878 (2019)
30. B.R. Lawn, D.B. Marshall, *J. Am. Ceram. Soc.* **62**(7–8), 347 (1979)
31. A. Moore, *Proc. R. Soc. Lond. Ser. A* **195**(1041), 231 (1948)
32. F.P. Bowden, D. Tabor, *The Friction and Lubrication of Solids*, Part II (Oxford University Press, Oxford, 1964)
33. J. Greenwood, G. Rowe, *J. Appl. Phys.* **36**(2), 667 (1965)
34. J.A. Schey, M. Shaw, *J. Tribol.* **3**(2), 173 (1984)
35. M.E. Merchant, *J. Appl. Phys.* **11**(3), 230 (1940)
36. M.P.F. Sutcliffe, "Surface Finish and Friction in Cold Metal Rolling," in *Metal Forming Science and Practice,* ed. by J.G. Lenard (Elsevier, Oxford, 2002), chap. 4, pp. 19–59
37. W.R. Wilson, W. Lee, *J. Manuf. Sci. Eng.* **123**(2), 279 (2001)
38. F. Larsson, "Surface Topography Measurements of Thin Aluminium Foil Transferred to FE-Smulations," Master's thesis, Lund University, Sweden (2016)
39. M. Odiotti, V. Colaprico, *Gravure Process and Technology* (Gravure Association of America, Gravure Education Foundation, 1991)
40. K. Osakada, M. Oyane, *Bull. JSME* **14**(68), 171 (1971)
41. D. Raabe, M. Sachtleber, H. Weiland, G. Scheele, Z. Zhao, *Acta Mater.* **51**(6), 1539 (2003)
42. R. Becker, *Acta Mater.* **46**(4), 1385 (1998)
43. N.K. Sundaram, Y. Guo, S. Chandrasekar, *Phys. Rev. Lett.* **109**(10), 106001 (2012)
44. F. Hashimoto, H. Yamaguchi, P. Krajnik, K. Wegener, R. Chaudhari, H.-W. Hoffmeister, F. Kuster, *CIRP Ann.* **65**(2), 597 (2016)
45. W.F. Hosford, R.M. Caddell, *Metal Forming: Mechanics and Metallurgy*, 4th edn. (Cambridge University Press, Cambridge, 2011)
46. R.N. Wright, *Metall. Mater. Trans. A* **3**(1), 83 (1972)
47. O. Wouters, W.P. Vellinga, R.V. Tijum, J.T.M. de Hosson, *Acta Mater.* **53**(15), 4043 (2005)
48. M. Zaiser, F.M. Grasset, V. Koutsos, E.C. Aifantis, *Phys. Rev. Lett.* **93**, 195507 (2004)
49. K.J. Stout, E. Davis, P. Sullivan, *Atlas of Machined Surfaces* (Springer, London, 2012)
50. A. Udupa, T. Sugihara, K. Viswanathan, S. Chandrasekar, *Phys. Rev. Appl.* **11**(1), 014021 (2019)
51. M. Buchanan, *Physics* **14**, 171 (2021)
52. L.E. Samuels, *Metallographic Polishing by Mechanical Methods*, 3rd edn. (ASM International, Materials Park, 1982)
53. L. Rayleigh, "The Ultimate Shape of Pebbles, Natural and Artificial," *Proc. R. Soc. London A, Math. Phys. Sci.* **181**(985) (Royal Society of London,1942), pp. 107–118
54. W.J. Firey,*Mathematika* **21**(1), 1 (1974)
55. D.J. Durian, H. Bideaud, P. Duringer, A. Schröder, F. Thalmann, C. Marques, *Phys. Rev. Lett.* **97**(2), 028001 (2006)
56. I.V. Kragelsky, M.N. Dobychin, V.S. Kombalov, *Friction and Wear: Calculation Methods* (Pergamon Press, Oxford, 1981)
57. E. Rabinowicz, *Friction and Wear of Materials* (Wiley, New York, 1995)
58. P. Stoyanov, J.M. Shockley, M. Dienwiebel, R.R. Chromik, *MRS Commun.* **6**(3), 301 (2016)
59. R. Aghababaei, D.H. Warner, J.-F. Molinari, *Proc. Natl. Acad. Sci. U.S.A.* **114**(30), 7935 (2017)
60. T. Sato, Z.B. Milne, M. Nomura, N. Sasaki, R.W. Carpick, H. Fujita, *Nat. Commun.* **13**, 2551 (2022)
61. R. Aghababaei, *Wear* **426–427**, 1076 (2019)
62. K. Zhao, R. Aghababaei, *J. Mech. Phys. Solids* **143**, 104069 (2020)
63. R. Aghababaei, T. Brink, J.-F. Molinari, *Phys. Rev. Lett.* **120**, 186105 (2018)
64. R. Aghababaei, *Phys. Rev. Mater.* **3**, 063604 (2019)
65. S. Pham-Ba, J.-F. Molinari, *Wear* **472**, 203648 (2021)
66. T. Brink, E. Milanese, J.-F. Molinari, *Phys. Rev. Mater.* **6**(1), 013606 (2022)
67. L. Brochard, S. Souguir, K. Sab, *Int. J. Fract.* **210**, 153 (2018)

Publisher's note

Ramin Aghababaei is an associate professor and Head of Section, Mechanics and Materials, in the Department of Mechanical and Production Engineering at Aarhus University, Denmark. With expertise in multiscale material modeling and computational tribology, he leads the Surface Mechanics and Tribology Laboratory. His research interests include numerical modeling of friction and wear phenomena as well as cutting processes, with a focus on the origins of material removal from solid surfaces. Aghababaei can be reached by email at ra@mpe.au.dk.

Emily E. Brodsky is an earthquake physicist at the University of California, Santa Cruz. She earned her AB degree from Harvard University in 1995, and her PhD degree in geophysics from the California Institute of Technology in 2001. She has published more than 130 peer-reviewed articles and been honored by the 2008 James B. Macelwane Medal from the American Geophysical Union (AGU), the 2021 Price Medal of the Royal Astronomical Society, and the 2022 Nemmers Prize in Earth Sciences, and is a Fellow of the AGU and the Geological Society of America. Brodsky can be reached by email at brodsky@ucsc.edu.

Jean-François Molinari is a French-Swiss engineer and scientist specializing in the numerical modeling of the mechanics of materials and structures. He is a full professor and the director of the Computational Solid Mechanics Laboratory at the École Polytechnique Fédérale de Lausanne, Switzerland. He is the chair of the Swiss Community for Computational Methods in Applied Sciences, and a member of the European Solid Mechanics Conference Committee (term of 2016–2021). He is editor-in-chief for *Mechanics of Materials*. Molinari can be reached by email at jean-francois.molinari@epfl.ch.

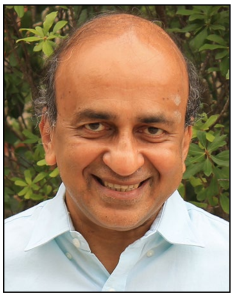

Srinivasan Chandrasekar is a professor in the Schools of Industrial Engineering and Materials Engineering, and director of the Center for Materials Processing and Tribology at Purdue University. His research and teaching interests focus on manufacturing, materials processing, structural materials, and tribology. His current research includes chemical effects in surface plasticity, energy efficient methods for producing sheet metals and powders, forming of natural materials, and nature of surfaces produced by manufacturing processes. Chandrasekar can be reached by email at chandy@purdue.edu.